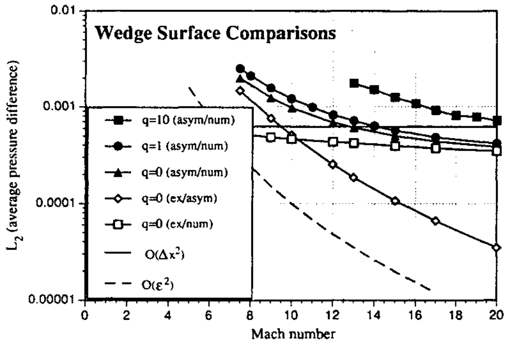

Fig. 2a Comparison along the wedge surface of exact, asymptotic, and numerical solutions using average pressure differences.

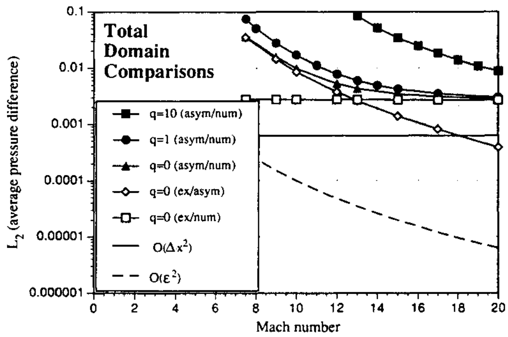

Fig. 2b Comparison over the entire domain of exact, asymptotic, and numerical solutions using average pressure differences.

shock due to inherent errors in the shock-capturing scheme and the error in the location of shock front predicted by the asymptotic method.

Calculations were first performed for $q = 0$ for $7.5 \leq M_0 \leq 20$. In this case the exact oblique shock solution is also available. From Fig. 2a, L_2 computed for the differences in the exact and numerical cases has a value near 4×10^{-4} which varies slowly with Mach number and is the same order of magnitude as the expected numerical error $[\mathcal{O}(\Delta x^2) = 6.25 \times 10^{-4}]$. L_2 was also computed for the differences between the asymptotic and exact solutions. As seen in Fig. 2a, this value of L_2 decreases with increasing Mach number, consistent with the asymptotic error estimate, which is $\mathcal{O}(\epsilon^2)$. L_2 is next calculated for the difference of the asymptotic and numerical methods with $q = 0$. At low supersonic Mach number, the difference is attributed to the error in the asymptotic method. For high Mach number, the difference is attributed to the error in the numerical method. A series of calculations was then performed for $q = 1$ and 10 over the same range of Mach numbers. For a given Mach number the value of L_2 increases with q. The curves follow the same trend as the $q = 0$ curve with increasing Mach number.

Final Remarks

Our results show that in addition to being useful as a means to gain basic understanding of high-speed reacting flows, asymptotic solutions of simple model problems are useful for making both qualitative and quantitative assessments of the numerical methods which are necessary for design of aerospace vehicles. By examining results which demonstrate the methods' basic agreement, such as those shown in Figs. 1a and 1b, additional confidence in the numerical method can be obtained. By studying results such as those shown in Figs. 2a and 2b, one can assess which approximation is responsible for the small differences that do exist. For example, the small differences in the results of Figs. 1a and 1b, obtained for $q = 10$, $M_0 = 20$, are primarily attributable to errors in the asymptotic method as seen in Figs. 2a and 2b. Nevertheless, the asymptotic solution shows that there is a nontrivial solution structure. Thus, one has a rational basis for distinguishing which structures predicted by the numerical method have a physical origin and which are numerical relics. As shown in detail in Ref. 3, as Mach number is held fixed and q is lowered, numerical errors overwhelm the effects of heat release so that the differences are primarily attributable to truncation errors in the numerical method.

In conclusion, it is recommended that the method of comparison given here be adopted as a new standard for numerical models of high-speed reacting flows.

Acknowledgments

This work was supported by the Jesse H. Jones Faculty Research Program and the NASA-ASEE Summer Faculty Fellowship Program. Thomas Jackson of Old Dominion University provided helpful suggestions for data presentation. The authors also thank Beverly Duncan and Shaye Yungster of NASA Lewis Research Center for assistance with the RPLUS code.

References

[1]Powers, J. M., and Stewart, D. S., "Approximate Solutions for Oblique Detonations in the Hypersonic Limit," *AIAA Journal,* Vol. 30, No. 3, 1992, pp. 726–736.

[2]Shuen, J.-S., and Yoon, S., "Numerical Study of Chemically Reacting Flows Using a Lower-Upper Symmetric Successive Overrelaxation Scheme," *AIAA Journal,* Vol. 27, No. 12, 1989, pp. 1752–1760.

[3]Powers, J. M., and Grismer, M. J., "Comparisons of Numerical and Exact Solutions for Oblique Detonations with Structure," AIAA Paper 91-1677, June 1991.

Supersonic Flutter of Composite Sandwich Panels

Le-Chung Shiau*
National Cheng Kung University, Tainan, Taiwan, Republic of China

Introduction

SANDWICH construction has been used in the aeronautical application for more than four decades since it offers the possibility of achieving high bending stiffness for small weight penalty. Today, there is renewed interest in using sandwich structures due to the introduction of new materials, such as advanced composite materials for the faces and nonmetallic honeycombs for core, which offer long awaited properties of both high stiffness and low specific weight. To use them efficiently a good understanding of their structural and dynamic behaviors under various loads is needed.

Panel flutter is a self-excited oscillation of the external skin of a flight vehicle and is caused by dynamic instability of inertia, elastic, and aerodynamic forces of the system. This type of aeroelastic instability has received much attention in the past 30 years.[1–4] As a result, this peculiar phenomenon is now reasonably understood for panels made of conventional isotropic materials. Recently, some works have been devoted to study the flutter characteristics of panels made of advanced composite materials,[5–8] but none of them deal with flutter of composite sandwich panels. In this Note, a flutter motion equation for a two-dimensional composite sandwich plate is derived by considering the total lateral displacement of the plate as the sum of the displacement due to bending of the

Received Nov. 21, 1991; revision received March 2, 1992; accepted for publication March 10, 1992.

*Professor, Institute of Aeronautics & Astronautics.

plate and that due to shear deformation of the core. The effects of core thickness and stacking sequence of the faces on the flutter boundary of the plate are discussed.

Mathematical Formulation

Consider a two-dimensional composite sandwich plate with length a, thickness h, and average mass density per unit volume ρ_m as shown in Fig. 1. The plate is assumed to consist of two symmetrical laminated face plates and an orthotropic honeycomb core. Supersonic airflow with air density ρ, flow velocity U, and Mach number M_∞ is assumed passing over the top surface of the plate along the positive x direction.

For sandwich construction having honeycomb core, it is reasonable to assume that the transverse normal stiffness of the core is infinitely large and the core makes no contribution to the bending and membrane stiffness of the sandwich plate. But the shear strains in the core of the sandwich plate need to be considered due to a low transverse modulus of rigidity of the core. With these assumptions and two-dimensional quasi-steady supersonic aerodynamic theory, the governing differential equations of motion for the two-dimensional sandwich plate can be derived as[9]

$$D_1\frac{\partial^4 w}{\partial x^4} - D_1\frac{\partial^3\gamma}{\partial x^3} + \rho_m h\frac{\partial^2 w}{\partial t^2} + \frac{\rho U^2}{\sqrt{M_\infty^2-1}}\left[\frac{\partial w}{\partial x} + \frac{M_\infty^2-2}{M_\infty^2-1}\frac{1}{U}\frac{\partial w}{\partial t}\right] = 0 \tag{1}$$

in which w is the lateral displacement of the plate, γ the average shear-strain angle of the plate, and D_1 the plate bending rigidity.

The total lateral displacement of the plate can be split into a partial deflection w_b due to bending and a partial deflection w_s due to shear. The two partial deflections can be related as[9]

$$\frac{\partial w_s}{\partial x} = -\frac{D_1}{S}\frac{\partial^3 w_b}{\partial x^3} \tag{2}$$

in which S is the transverse shear stiffness and given by $S = cG_{xz}$ where G_{xz} is the transverse shear modulus of the core and c is the core thickness.

Substituting Eq. (2) into Eq. (1), one obtains

$$D_1\frac{\partial^4 w_b}{\partial x^4} + \rho_m h\frac{\partial^2 w_b}{\partial t^2} - \rho_m h\frac{D_1}{S}\frac{\partial^4 w_b}{\partial x^2\partial t^2} + \frac{\rho U^2}{\sqrt{M_\infty^2-1}}\left[\frac{\partial w_b}{\partial x} - \frac{D_1}{S}\frac{\partial^3 w_b}{\partial x^3} + \frac{M_\infty^2-2}{M_\infty^2-1}\frac{1}{U}\frac{\partial w_b}{\partial t} - \frac{M_\infty^2-2}{M_\infty^2-1}\frac{D_1}{US}\frac{\partial^3 w_b}{\partial x^2\partial t}\right] = 0 \tag{3}$$

Assuming the displacements of the plate are exponential functions of time, $w_b = \bar{w}_b(x)\,e^{i\omega t}$, and introducing the following nondimensional parameters and constants

$$W_b = \bar{w}_b/h \qquad \xi = x/a \qquad k = \omega/\omega_0 \qquad \lambda = \frac{\rho U^2 a^3}{\sqrt{M_\infty^2-1}D}$$

$$g = \frac{\rho U}{M_\infty \rho_m h\,\omega_0} \qquad \omega_0 = \pi^2\sqrt{\frac{D}{\rho_m h a^4}} \qquad Z = k^2 - ikg$$

Equation (3) can be nondimensionalized as

$$\frac{D_1}{D}\frac{\partial^4 W_b}{\partial\xi^4} - \frac{\lambda D_1}{Sa^2}\frac{\partial^3 W_b}{\partial\xi^3} + \frac{D_1}{Sa^2}\pi^4 Z\frac{\partial^2 W_b}{\partial\xi^2} + \lambda\frac{\partial W_b}{\partial\xi} + \pi^4 Z W_b = 0 \tag{4}$$

in which λ is the nondimensional aerodynamic pressure, k the nondimensional frequency, and D the bending stiffness of the plate when all fibers are aligned with the x axis.

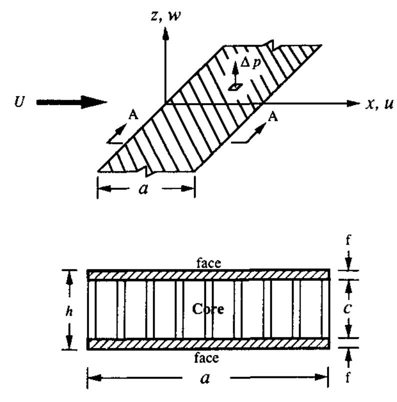

Fig. 1 Sandwich panel geometry.

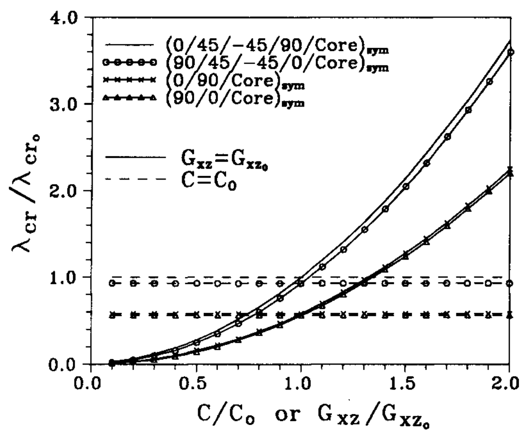

Fig. 2 Effects of C and G_{xz} on flutter boundary.

The solutions to Eq. (4) have the form

$$W_b = \sum_{j=1}^{4} C_j e^{b_j\xi} \tag{5}$$

where b_j are the roots of the polynomial

$$\frac{D_1}{D}b^4 - \frac{\lambda D_1}{Sa^2}b^3 + \frac{D_1}{Sa^2}\pi^4 Z b^2 + \lambda b - \pi^4 Z = 0 \tag{6}$$

Equation (5) possesses four unknown constants so that four boundary conditions are required. For the two-dimensional sandwich plate with simply supported edges, the boundary conditions are as follows:

$$\text{at } x = 0 \qquad w(0) = \frac{\partial^2 w(0)}{\partial x^2} = 0 \tag{7a}$$

$$\text{at } x = a \qquad w(a) = \frac{\partial^2 w(a)}{\partial x^2} = 0 \tag{7b}$$

Satisfaction of the boundary conditions by substituting Eq. (5) into Eq. (7) gives four homogeneous, linear algebraic equations in the unknowns C_j. Setting the determinant of coefficients equal to zero gives the characteristic equation for the eigenvalues. The functional relation may be expressed as

$$H(\lambda, Z) = 0 \tag{8}$$

For a given λ and Z, the four roots in Eq. (6) can be determined and the complex function H is evaluated. In general, H will not be zero, and so another value of Z is chosen for the fixed λ and H is recomputed until a zero of H is obtained with acceptable accuracy. For low values of λ, the eigenvalues Z are real. As the flow velocity increases from zero, two eigenvalues will usually approach each other and

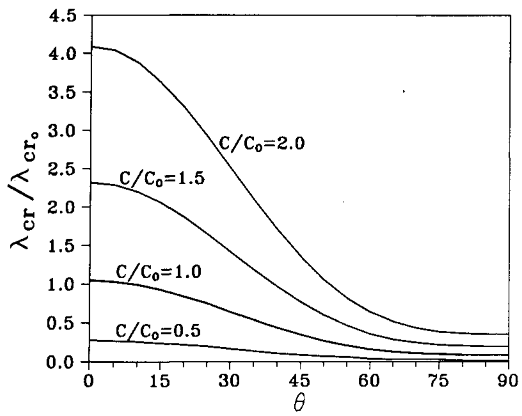

Fig. 3 Effects of fiber orientation on flutter boundary.

coalesce to Z_{cr} at a value of $\lambda = \lambda_{cr}$, which is a critical value of dynamic pressure, and become a complex conjugate pair for $\lambda > \lambda_{cr}$. The solution procedures used here represent an exact solution rather than a modal solution of the differential equation and hence do not possess convergence difficulties.

Numerical Results

The panel considered for the analysis is a $[0/\pm 45/90/\text{Core}]_{sym}$ sandwich plate. AS4/3501-6 graphite epoxy is used for the face sheets and Al honeycomb is used for the core. The material constants are $E_2 = 10{,}130$ N/mm^2, $E_1 = 11.45E_2$, $G_{12} = 0.543E_2$, $\nu_{12} = 0.3$ for the face sheets, and $G_{xz} = 0.0429E_2$ for the core. The thickness of each lamina is 0.125 mm. The core thickness is set to be 10 mm. Figure 2 shows the effects of thickness and transverse shear modulus of the core on the flutter boundary of the panels with four different stacking sequencies. All flutter boundaries have been normalized to $\lambda_{cr_0} = 155.9$ of the $[0/\pm 45/90/\text{Core}]_{sym}$ panel with $c_0 = 10$ mm and $G_{xz_0} = 0.0429E_2$. The solid lines represent cases with $G_{xz} = G_{xz_0}$ and dashed lines represent cases with $c = c_0$. It shows that G_{xz} has negligible effect on the flutter boundaries since changing G_{xz} with fixed c will not affect the bending stiffness of the plate which governs the flutter boundary. But changing c with fixed G_{xz} will have pronounced effect on the flutter boundary since the bending stiffness of the plate is mainly dependent on the core thickness. Furthermore, with the same number of lamina and fiber orientation, the stacking sequence of the face sheets has small effect on the flutter boundary. Figure 3 shows the effect of fiber orientation on the flutter boundary of $[\pm\theta/\text{Core}]_{sym}$ sandwich panels (λ_{cr} is also normalized to λ_{cr_0} of the $[0/\pm 45/90/\text{Core}]_{sym}$ panel). For all different core thickness, the highest flutter boundary is obtained with the fiber aligned with the x axis; rotating the fiber away from the x axis results in a continuous reduction in flutter boundary for values of θ up to 90 deg.

Conclusions

A flutter motion equation for a two-dimensional composite sandwich panel is derived by considering the total lateral displacement as the sum of the displacement due to bending of the plate and that due to shear deformation of the core. The aerodynamic theory is based on the piston theory with first-order approximation. The Mach number considered is limited to beyond approximately 1.6. This derivation can be extended to the general composite sandwich panel system for practical application in the aeronautical industry. The results show that the composite sandwich panel greatly improves the flutter boundary over the corresponding composite laminated panel if it has a proper core thickness. The results also show that the transverse shear G_{xz} of the core has negligible effects on flutter boundaries.

References

[1]Calligeros, J. M., and Dugundji, J., "Effects of Orthotropicity Orientation on Supersonic Panel Flutter," *AIAA Journal*, Vol. 1, No. 9, 1963, pp. 2180–2182.

[2]Ventres, C. S., and Dowell, E. H., "Comparison of Theory and Experiment for Nonlinear Flutter of Loaded Plates," *AIAA Journal*, Vol. 8, No. 11, 1970, pp. 2022–2030.

[3]Mei, C., "A Finite Element Approach for Nonlinear Panel Flutter," *AIAA Journal*, Vol. 15, No. 8, 1977, pp. 1107–1110.

[4]Han, A. D., and Yang, T. Y., "Nonlinear Panel Flutter Using High-Order Triangular Finite Element," *AIAA Journal*, Vol. 21, No. 10, 1983, pp. 1453-1461.

[5]Rossettos, J. W., and Tong, P., "Finite Element Analysis of Vibration and Flutter of Cantilever Anisotropic Plates," *Journal of Applied Mechanics*, No. 4, 1974, pp. 1075–1080.

[6]Sawyer, J. W., "Flutter and Buckling of General Laminated Plates," *Journal of Aircraft*, Vol. 14, No. 4, 1977, pp. 387–393.

[7]Shiau, L. C., and Lu, L. T., "Nonlinear Flutter of Two-Dimensional Simply Supported Symmetric Composite Laminated Plates," *Journal of Aircraft*, Vol. 29, No. 1, 1992, pp. 140–145.

[8]Shiau, L. C., and Chang, J. T., "Transverse Shear Effect on Flutter of Composite Panels," *Journal of Aerospace Engineering*, Vol. 5, No. 4, 1992, pp. 465–479.

[9]Plantema, F. J., *Sandwich Construction*, Wiley, New York, 1966, pp. 3–5.

Criterion for Decoupling Dynamic Equations of Motion of Linear Gyroscopic Systems

M. Liu* and J. M. Wilson†
University of Durham,
Durham DH1 3LE, England, United Kingdom

I. Introduction

THE damping matrix of a general linear structural vibration system is a very important physical parameter in describing the differential equations of motion of the system. In analyzing the dynamic responses of such a system, the damping term should never be neglected. In the case of the general damping matrix, which consists of conventional damping and gyroscopic damping and can be expressed in terms of symmetrical and nonsymmetrical matrices,[1] the system equations of motion can seldom be decoupled in their corresponding real mode space. Therefore, complex modal theories are conventionally employed to perform a dynamic analysis of the system. This makes the analyses and computations much more complicated than necessary. In this Note, a system with general damping is changed to an undamped one using a transformation matrix of function in general coordinates. The obtained undamped system is not equivalent to that of a decoupled one in the real mode space. The necessary and sufficient condition for this transformation is derived. As a consequence, the Caughey's condition, which is necessary and sufficient to decouple the dynamic equations of motion of a symmetrical linear damped system in terms of the classical real modes, is extended to nonsymmetrical systems.

II. Basic Equations

For a linear structural vibration system with a general form of nonsymmetric damping matrix denoted by $\ll M, C, K \gg$, its differential equations of motion take the following form:

$$[M]\{\ddot{x}\} + [C]\{\dot{x}\} + [K]\{x\} = \{f(t)\} \tag{1}$$

Received Aug. 8, 1991; revision received April 14, 1992; accepted for publication April 27, 1992.

*Lecturer from Jilin University of Technology, PRC; currently, Research Fellow, School of Mechanical and Offshore Engineering, Robert Gordon University, Aberdeen, Scotland, UK.

†Lecturer, School of Engineering and Applied Science.